



**Performance Evaluation of Azista Drifter Buoys Deployed by INCOIS
in the Indian Ocean During 2024-2025**

By

Ashin, K., Girishkumar, M. S., Rajesh, K., Karthika P. S., Suresh Kumar, N., Sai
Theagarajan, Venkat Shesu, R., Murali Krishan, A., Aneesh Lotliker, E. Pattabhi Rama
Rao

Indian National Centre for Ocean Information Services (INCOIS)

Earth System Science Organization (ESSO)

Ministry of Earth Sciences

Hyderabad, India

August 2025

DOCUMENT CONTROL SHEET

Earth System Science Organization (ESSO)

Ministry of Earth Sciences (MoES)

Indian National Centre for Ocean Information Services (INCOIS)

ESSO Document Number: ESSO-INCOIS-OMDA-TR-06(2025)

Title of the report: Performance Evaluation of Azista Drifter Buoys Deployed by INCOIS in the Indian Ocean During 2024-2025

Author(s): Ashin, K., Girishkumar, M. S., Rajesh, K., Karthika P. S., Suresh Kumar, N., Sai Theagarajan, Venkat Shesu, R., Murali Krishan, A., Aneesh Lotliker, E. Pattabhi Rama Rao

Originating unit: Ocean Observation Network Division (OON), INCOIS.

Type of Document: Technical Report (TR)

Number of pages and figures: 39 pages, 21 figures, and 3 tables

Number of references: 17

Keywords: Drifter buoys, Sea Surface Temperature, Barometric Pressure

Security classification: Open

Distribution: Open

Date of publication: 14 August 2025

Abstract

Between October 2024 and March 2025, the Indian National Centre for Ocean Information Services (INCOIS) deployed nine drifters from Azista Aerospace in the eastern Arabian Sea to collect sea surface temperature (SST) and barometric pressure data. Despite the intended objectives, these drifters encountered multiple operational and data quality issues. One unit (DB18) failed immediately after deployment, and another (DB24), deployed south of the equator, reported erroneous locations north of the equator. After filtering invalid Global Positioning System (GPS) coordinates and speeds exceeding 3 m s^{-1} , usable tracks were recovered from seven drifters (DB17, DB20–DB23, DB25–DB26), with operational durations ranging from 16 to 163 days, before it failed in the open ocean region. As of April 2025, three drifters (DB17, DB20, and DB21) remained active, while the remaining four ceased data transmission earlier. After applying to basic quality control procedure to drifter measurements, such as spike test, geographical location error, sensor range test and drifter speed test, percentage of retained data ranged from 50.4% (DB21) to 92.9% (DB23). Sensor validation using satellite based daily gridded SST field and ERA5 barometric pressure datasets revealed mixed performance. SST correlations ranged from 0.83 to 0.99 for most buoys, except DB23 (0.48), while RMSD values exceeded 0.7°C for all but DB20 (0.24°C), and DB21 showed unrealistic SST peaks even after filtering. Pressure data showed generally strong correlations (0.72–0.97), but barometric pressure RMSD values varied widely, from 0.32 to 1.58 hPa. DB17, DB20, and DB21 exhibited unrealistic diurnal noise in barometric pressure measurements from the drifter. In contrast, DB22 and DB23 demonstrated good agreement with ERA5, despite their short operational lifetimes.



Performance Evaluation of Azista Drifter Buoys Deployed by INCOIS in the Indian Ocean During 2024-2025

By

Ashin, K., Girishkumar, M. S., Rajesh, K., Karthika P. S., Suresh Kumar, N., Sai Theagarajan, Venkat Shesu, R., Murali Krishan, A., Aneesh Lotliker, E. Pattabhi Rama Rao

Indian National Centre for Ocean Information Services (INCOIS)

Earth System Science Organization (ESSO)

Ministry of Earth Sciences

Hyderabad, India

June 2025

Acknowledgment

The encouragement provided by the Director, INCOIS, is gratefully acknowledged. We sincerely thank the Vessel Management Cells (VMC) at NIOT; Mr. Subramaniam M. M. from NCPOR; Dr. Arul M.; and his colleagues from the Ocean Observation System group, NIOT, specifically Thirumurugan for their valuable support in the deployment of floats during various field campaigns. The authors thank two reviewers, Dr. P. A. Maheswaran, Scientist-F, NPOL, DRDO, and Dr. Jossia J., Scientist-F, NIOT, MoES, for their extensive and constructive comments and suggestions, which greatly helped to improve the manuscript.

Contents

Abstract	3
Acknowledgment.....	6
1. Introduction	8
2. Methodology.....	10
2.1. Deployment Details.....	10
2.2. Data Processing and Filtering	10
2.2.1. Coordinate Filtering	10
2.2.2. Speed Filtering	11
2.2.3. Sea Surface Temperature (SST) Filtering	11
2.2.4. Barometric Pressure (BP) Filtering	11
2.3. Data Validation	12
3. Results and discussion	13
3.1. Operational Lifespan and Reliability	13
3.2. GPS Data Validation	14
3.3. Temperature and Barometric Pressure Filtering.....	15
3.4 Evaluation of SST and BP from Drifter	15
4. Summary.....	17

1. Introduction

Surface drifting buoys is vital component of in the global ocean observing system, providing high-resolution, real-time measurements of sea surface temperature (SST), barometric pressure (BP), and near-surface ocean currents (Lumpkin and Pazos, 2007). These autonomous instruments, designed to drift with prevailing ocean circulation, provide a critical data for numerical weather prediction, climate monitoring, and marine hazard forecasting by supplementing satellite observations with in-situ measurements (Lumpkin and Pazos, 2007; Elipot et al., 2016; Lumpkin et al., 2013). In regions such as the Indian Ocean characterized by strong monsoonal variability, and complex air–sea interactions, drifter data are particularly valuable for thereanalysis models and supporting operational oceanography.

Drifter data also play a key role in advancing our understanding of high-frequency and small-scale oceanic processes, including inertial oscillations, tides, and submesoscale vortices (Elipot and Lumpkin, 2008; Elipot et al., 2010; Chaigneau et al., 2008; Lumpkin and Elipot, 2010; Poulain and Centurioni, 2015). Moreover, accurate and reliable SST and BP measurements from drifters contribute not only to short-term forecasting but also to the long-term development of climatologies (Castro et al., 2012).

In addition to supporting physical oceanography, knowledge of near-surface currents derived from drifter observations has broad utility. Applications include search and rescue operations, biogeochemical studies, and both hindcast and forecast models of the transport and dispersion of floating materials such as plastic debris and oil spills (McCord et al., 1999; Davidson et al., 2009; Yoder et al., 1994; Law et al., 2010; Maximenko et al., 2012).

To enhance observational capacity in Indian waters, the Indian National Centre for Ocean Information Services (INCOIS) procured ten indigenously developed drifter buoys by Azista BST Aerospace (AZDB series). These buoys were equipped with sensors for SST and BP, along with onboard Global Positioning System (GPS) and INSAT-based telemetry to ensure regular data transmission in every one hour interval. Between 2024 and 2025, nine of the ten buoys were deployed in various regions of the Indian Ocean with the objective of augmenting routine monitoring and assessing the performance of the Azista drifter under various oceanographic and atmospheric conditions. Despite rigorous pre-deployment test at INCOIS and onboard research vessels, initial data quality varied across the deployments. This underscores the importance of systematic evaluation and validation against independent datasets to evaluate the overall performance of drifter, a practice routinely followed in global drifter programs (Carval, 2022). Such an exercise will provide critical guidance for future procurement decisions, operational planning, and improvement of observational strategies.

This report presents a detailed evaluation of the deployment, operational performance, and data quality of the Azista drifter buoys. It also outlines the data processing methodologies and validation procedures used, and provides recommendations for enhancing the reliability and utility of these platforms in future observational efforts.

2. Methodology

2.1. Deployment Details

INCOIS deployed nine Azista drifter buoys in the Indian Ocean between October 2024 and March 2025, with deployment locations primarily ranging between 12°N and 19°N latitude and 67°E to 69°E longitude (Table 1). One additional buoy (DB24) was deployed in the southern hemisphere at 1.48°S, 80.47°E. All buoys were equipped with GPS and INSAT communication systems and pre-deployment test were carried at INCOIS and also at onboard research vessels to verify sensor functionality and transmission capability. A spatial map of deployment locations and initial drifter trajectories is shown in Figure 1.

2.2. Data Processing and Filtering

The initial dataset included GPS coordinates, sea surface temperature (SST), and barometric pressure (BP) recorded at a nominal sampling interval of one hour. Following Carval (2022), a series of filtering procedures were applied to remove erroneous or physically implausible values prior to further analysis, and it is summarized below.

2.2.1. Coordinate Filtering

All position data were screened to eliminate coordinates falling on land or outside valid geospatial bounds. This step removed transmission errors and nonphysical drifter locations from the trajectory records. The raw drifter gps data is shown in Figure 2.

2.2.2. Speed Filtering

To ensure the accuracy of surface trajectories, a speed-based quality control check was applied to identify and remove implausible GPS fixes. Drift speeds were computed using sequential positions and timestamps, taking into account actual position acquisition times. Although ocean surface currents can vary regionally drift speeds exceeding 3 m s^{-1} are considered physically unrealistic for free-drifting buoys. Values above this threshold typically indicate erroneous position or timestamp entries, or possibly mislabeled or duplicated data. Data points corresponding to speeds exceeding 3 m/s were discarded (Carval, 2022).

2.2.3. Sea Surface Temperature (SST) Filtering

Two stages of filtering were applied to the SST data as follows. SST values outside the physical range of $+10^{\circ}\text{C}$ to $+35^{\circ}\text{C}$ were removed, based on the operational limits of the temperature sensor. In addition, a 24-hour moving window was applied to identify and eliminate spikes. Values exceeding ± 3 standard deviations from the median within the window were flagged and excluded.

2.2.4. Barometric Pressure (BP) Filtering

Pressure data were subjected to two levels of quality control. First, a range filter was applied to discard BP values falling outside the plausible atmospheric pressure range of 850 to 1055 hPa. Following this, a 24-hour moving median filter was implemented to identify and remove outliers

exceeding three standard deviations from the median, consistent with the method used for SST filtering.

A geographic map of all raw drifter positions is shown in Figure 2, illustrating the extent of the initial dataset prior to filtering. After the filtering procedures, usable tracks were retained for seven drifters (DB17, DB20–DB23, DB25–DB26). These filtered trajectories are shown in Figure 2 (referenced in the Deployment Details section), with each drifter plotted in a unique color for clarity. Representative examples of the SST and BP filtering process are provided in Figures 3 and 4, respectively.

2.3. Data Validation

The accuracy of SST and BP measurements recorded by the Azista drifter buoys was assessed through comparison with independent reference datasets. Filtered SST data were averaged to daily resolution and evaluated against optimally interpolated (OI) Version 5 SST product from Remote Sensing Systems (REMSS), which is derived from multi-mission microwave and infrared (MW_IR) satellite sensors and provides daily fields at a spatial resolution of 0.09° (Gentemann et al., 2003). For BP validation, hourly mean sea level pressure (MSLP) measurements from the drifters were compared with the ERA5 reanalysis dataset, produced by the European Centre for Medium-Range Weather Forecasts, which offers global hourly pressure fields at 0.25° spatial resolution (Hersbach et al., 2020).

To quantify agreement between the drifter and reference datasets, standard statistical metrics were computed, including the correlation coefficient, root mean square deviation (RMSD), and standard deviation. These comparisons provided a quantitative basis for evaluating sensor fidelity across deployments and time periods. Due to the lack of collocated in situ buoy measurements,

satellite-based SST products and reanalysis-based surface pressure fields served as the principal sources for validation.

3. Results and discussion

3.1. Operational Lifespan and Reliability

The operational lifespan and data return rates of the nine Azista drifter buoys deployed by INCOIS between October 2024 and March 2025 provide a first-order assessment of their field reliability. Table 1 summarizes key deployment parameters, including duration of operation and the percentage of data received.

Out of the nine units deployed, seven buoys (DB17, DB20–DB23, DB25, and DB26) returned data, with durations ranging from 16 days (DB23) to 163 days (DB17) (Figure 5). Among these, three buoys (DB17, DB20, and DB21) were still transmitting data as of 7 April 2025, having remained operational for 163, 33, and 161 days, respectively. These buoys also exhibited relatively high data return rates (DB17: 89.90%, DB20: 93.50%, and DB21: 77.08%) , based on the expected one-hourly transmission interval (Figure 6).

The remaining four buoys had generally shorter lifespans DB22 operated for 23 days with a data return rate of 93.47%, and DB23 for 16 days with 77.62%. DB25 functioned for 30 days, achieving 81.00% data return. DB26, although active for 137 days, returned only 10.20% usable data, one of the lowest among the fleet (Table 1; Figures 5 and 6).

Two buoys failed to provide valid data. DB18 failed immediately upon deployment, transmitting no usable data. DB24, deployed south of the equator at 1.48°S, consistently reported erroneous GPS positions in the northern hemisphere. Due to these corrupted coordinates, its dataset was excluded from analysis.

Battery voltage measurements remained stable (approximately 12V) throughout all deployments. Additionally, no indications of beaching, or vandalism were observed during or after deployment.

3.2. GPS Data Validation

The quality and reliability of the GPS-derived positions were evaluated following the filtering procedures described in Section 2.2. Specifically, data points falling outside valid geographic boundaries and those associated with unrealistically high speeds (>3 m/s) were removed. The percentages of retained data after each filtering step, calculated relative to the total received data, are summarized in Table 2 and Figure 7.

Most buoys demonstrated high GPS integrity, such as DB17, DB20, DB22, and DB23 retained over 95% data after removing both erroneous GPS position and drift speed of magnitude 3 ms^{-1} . DB25 also performed reasonably well, with 84.8% of its data preserved. In contrast, DB26 exhibited much degraded performance, retaining 74.4% after applying GPS filtering and 70.2% after drift speed filtering. DB21 returned only 53.8% of the received data after applying GPS filtering and drift speed (Figure 7).

These differences reflect variability in both GPS performance and transmission stability across the Azista drifter units. Nonetheless, the filtered data were sufficient to reconstruct reliable surface tracks for most buoys, as exhibited in Figure 1.

3.3. Temperature and Barometric Pressure Filtering

The SST and BP datasets further quality controlled as described in Section 2.2, with range and spike filters applied to remove unrealistic values. The percentage of valid data retained after each filtering stage based on the received data is summarized in Table 2 and Figure 7.

Among the seven buoys with usable tracks, DB17, DB20, DB22, and DB23 retained over 90% of their SST and BP measurements. DB25 showed moderate retention (~74% for SST, 72% for BP), while DB26 and DB21 exhibited the lowest return and retained approximately 64% and 51% of SST data, respectively. Pressure data followed a similar trend, with DB26 showing only 53.6% retention (Figure 7).

These variations in sensor performance, despite similar deployment protocols, underscore the need for improved quality control during production and pre-deployment calibration.

3.4 Evaluation of SST and BP from Drifter

After applying to basic quality control procedures to drifter measurements, such as spike test, geographical location error, sensor range test, and drifter speed test, we evaluated the SST and BP measurements from the Azista drifters using MW IR OI SST and ERA5 MSLP datasets,

respectively (Section 2.3). Metrics such as the correlation coefficient, RMSD, and STD were used to quantify sensor performance (Table 3).

Most drifters exhibited a strong correlation with reference SST data, with values ranging from 0.83 to 0.99, except for DB23, which showed a notably low correlation of 0.48 (Figure 8-14). However, RMSD values for SST were relatively high in most cases, exceeding 0.7°C for all drifters except DB20, whose SST RMSD was 0.24°C (Figure 9). In contrast, the Marlin-Yug drifter buoy evaluated in a previous INCOIS study demonstrated SST RMSD values consistently below 0.4°C , indicating better agreement with satellite-derived SST (Karthika et al., 2025). Most of the drifters (DB17, DB22, DB23, DB25, and DB26) exhibited systematic biases in their SST measurements when compared to MWIR, suggesting consistent sensor calibration offsets. DB21, however, differed from this pattern by displaying frequent unrealistic peaks and high-frequency noise in the SST time series, even after the application of quality control filters. Despite these issues, the standard deviations of the SST data from all drifters were generally in agreement with those of the MWIR dataset, indicating that the overall variability was captured reasonably well.

BP comparisons revealed mixed performance. While correlation coefficients were generally high (0.72–0.97), RMSD values varied from 0.32 to 1.58 hPa. DB17, had the poorest BP performance with an RMSD of 1.58 hPa and visible unrealistic diurnal variability (Table 3, Figure 15-21). Similar issues were observed in DB20 and DB21, both of which showed elevated RMSD (1.55 and 0.89 hPa) with unrealistic diurnal variability (Figure 17-18). In contrast, DB22 and DB23, despite operating for only 23 and 16 days, respectively, achieved excellent agreement with ERA5, with RMSD values below 0.4 hPa and high correlation (0.97) (Figure 18-19). The standard deviations of the drifter BP data were, in most cases, consistent with ERA5. However, DB26 had limited usable data and could not be evaluated.

Although the basic quality control procedure successfully returned significant data, most of the buoys continued to exhibit data quality issues, especially in the form of diurnal noise in BP and high bias in SST of magnitude 1C. These findings point to persistent sensor calibration inconsistencies or internal electronic errors, necessitating further improvements in the Azista drifter design for reliable long-term deployment.

4. Summary

This report presents the deployment, data processing, and performance evaluation of nine Azista drifter buoys deployed by INCOIS in the eastern Arabian Sea between October 2024 and March 2025. Of the ten procured units, nine were deployed; one unit (DB18) failed immediately upon deployment, and another (DB24), deployed south of the equator, returned invalid GPS positions north of the equator. These two units were excluded from further analysis. The remaining seven drifters (DB17, DB20–DB23, DB25, and DB26) returned varying amounts of usable data and were evaluated in detail.

A systematic quality control procedure described in Section 2 was implemented to remove erroneous GPS coordinates, unrealistic speeds (threshold >3 m/s), and spurious sea surface temperature (SST) and barometric pressure (BP) readings. After GPS and speed filtering, the percentage of retained data ranged from 53.8% (DB21) to 97% (DB17, and DB20). Subsequent temperature and pressure filters further reduced usable data, with final post-QC retention ranging from 50.4% (DB21) to 92.9% (DB23), highlighting considerable variability in data quality across the drifters.

Sensor validation was carried out by comparing SST data with daily MW IR OI SST and BP data with hourly ERA5 reanalysis. Most drifters showed high SST correlation values (0.83–0.99), except DB23 (0.48). However, RMSD values exceeded 0.7°C for most units, indicating systematic biases in SST measurements. DB20 was an exception, with an RMSD of 0.24°C and stable performance. DB21, by contrast, exhibited unrealistic SST peaks even after filtering, suggesting faulty sensor behavior.

Barometric pressure sensors showed moderate-to-strong correlation with ERA5 data (0.72–0.97), but RMSD values varied from 0.32 hPa to 1.58 hPa. DB17, DB20, and DB21 exhibited unrealistic diurnal variability in BP, pointing to potential electronic noise or calibration drift. In contrast, DB22 and DB23, despite shorter lifespans, showed excellent agreement with ERA5 (RMSD <0.4 hPa). DB26 had limited usable data for validation and was not considered reliable.

In summary, the evaluation shows significant inconsistencies in data quality and sensor performance among the deployed Azista drifters. While some units, such as DB20 and DB22, performed well, many experienced systematic measurement errors, noisy signals, or early failure. Operational lifespans varied widely, from 16 to 163 days, with only three units (DB17, DB20, and DB21) still active as of April 2025. Several anomalies in SST and BP were present from the start of transmission, indicating possible pre-existing sensor issues. Although the MW IR SST and ERA5 BP datasets used for validation have spatial and temporal limitations, their agreement with independent Marlin-Yug drifter observations supports their use as reference datasets in this analysis. These results highlight the need for stronger pre-deployment protocols, including rigorous calibration, drift characterization under controlled conditions, and short-term coastal or harbor trials with inter-comparison against calibrated reference sensors. Implementing these measures, as recommended to the manufacturer, is expected to improve sensor reliability, extend

operational lifespans, and enhance the suitability of Azista drifters for sustained oceanographic and meteorological observations.

Appendix: The reason for the delay in the deployment of drifters after receiving at INCOIS.

Until June 19 2024, INCOIS was receiving real-time data via the INSAT-3D satellite. Following the satellite's end-of-life status, real-time data reception at the INCOIS Hub was disrupted. The issue was promptly escalated to ISRO, which subsequently allocated temporary carriers on the INSAT-3DS satellite. However, initial testing using INSAT-3DS revealed significant data gaps in real-time transmissions from drifters. These technical issues were communicated in detail to ISRO, SCNP, and MCF. After sustained follow-up by INCOIS, ISRO allocated a carrier on the GSAT-17 satellite for testing on July 23, 2024. This necessitated firmware updates to the Azista drifters to ensure compatibility with the new satellite configuration. Following extensive collaboration between the INCOIS and Azista teams, the firmware was successfully updated, and data reception has since resumed reliably. This transition process, however, caused delays in the immediate deployment of drifters upon their arrival at INCOIS.

References

- Castro, S. L., Wick, G. A., & Emery, W. J. (2012). Evaluation of the relative performance of sea surface temperature measurements from different types of drifting and moored buoys using satellite-derived reference products. *Journal of Geophysical Research: Oceans*, 117(C2). <https://doi.org/10.1029/2011JC007034>
- Chaigneau, A., Pizarro, O., & Rojas, W. (2008). Global climatology of near-inertial current characteristics from Lagrangian observations. *Geophysical Research Letters*, 35, L13603. <https://doi.org/10.1029/2008GL034060>
- Davidson, F. J. M., et al. (2009). Applications of GODAE ocean current forecasts to search and rescue and ship routing. *Oceanography*, 22(3), 176–181. <https://doi.org/10.5670/oceanog.2009.76>
- Elipot, S., & Lumpkin, R. (2008). Spectral description of oceanic near-surface variability. *Geophysical Research Letters*, 35, L05606. <https://doi.org/10.1029/2007GL032874>

Elipot, S., Lumpkin, R., & Prieto, G. (2010). Modification of inertial oscillations by the mesoscale eddy field. *Journal of Geophysical Research: Oceans*, 115, C09010. <https://doi.org/10.1029/2009JC005679>

Gentemann, C. L., Chelton, D. B., & Wentz, F. J. (2003). Diurnal signals in satellite sea surface temperature measurements. *Geophysical Research Letters*, 30(3), 1140. <https://doi.org/10.1029/2002GL016291>

Hersbach, H., Bell, B., Berrisford, P., Hirahara, S., Horányi, A., Muñoz-Sabater, J., Nicolas, J., Peubey, C., Radu, R., Schepers, D., Simmons, A., Soci, C., Abdalla, S., Abellan, X., Balsamo, G., Bechtold, P., Biavati, G., Bidlot, J., Bonavita, M., ... Thépaut, J. N. (2020). The ERA5 global reanalysis. *Quarterly Journal of the Royal Meteorological Society*, 146(730), 1999–2049. <https://doi.org/10.1002/qj.3803>

Karthika, P. S., Girishkumar, M. S., Ashin, K., Jeyakumar, C., Sherin, V. R., Suresh Kumar, Sai Theagarajan, Lotliker, A., & Pattabhi Rama Rao, E. (2025). Evaluation of overall performance and measurements from Marlin-Yug drifting buoy in the northern Indian Ocean during 2021–2024. INCOIS Technical Report

Law, K. L., Morét-Ferguson, S., Maximenko, N. A., Proskurowski, G., Peacock, E. E., Hafner, J., & Reddy, C. M. (2010). Plastic accumulation in the North Atlantic Subtropical Gyre. *Science*, 329(5996), 1185–1188. <https://doi.org/10.1126/science.1192321>

Lumpkin, R., & Elipot, S. (2010). Surface drifter pair spreading in the North Atlantic. *Journal of Geophysical Research: Oceans*, 115, C12017. <https://doi.org/10.1029/2010JC006338>

Lumpkin, R., Grodsky, S. A., Centurioni, L., Rio, M.-H., Carton, J. A., & Lee, D. (2013). Removing spurious low-frequency variability in drifter velocities. *Journal of Atmospheric and Oceanic Technology*, 30(2), 353–360. <https://doi.org/10.1175/JTECH-D-12-00139.1>

Lumpkin, R., & Pazos, M. (2007). Measuring surface currents with SVP drifters: The instrument, its data, and some recent results. In A. Griffa, A. D. Kirwan Jr., A. J. Mariano, T. Özgökmen, & H. T. Rossby (Eds.), *Lagrangian Analysis and Prediction of Coastal and Ocean Dynamics* (pp. 39–67). Cambridge University Press.

Maximenko, N., Hafner, J., & Niiler, P. (2012). Pathways of marine debris derived from trajectories of Lagrangian drifters. *Marine Pollution Bulletin*, 65(1–3), 51–62. <https://doi.org/10.1016/j.marpolbul.2011.04.016>

McCord, M. R., Lee, Y. K., & Lo, H. K. (1999). Ship routing through altimetry-derived ocean currents. *Transportation Science*, 33(1), 49–67. <https://doi.org/10.1287/trsc.33.1.49>

Poulain, P.-M., & Centurioni, L. (2015). Direct measurements of world ocean tidal currents with surface drifters. *Journal of Geophysical Research: Oceans*, 120, 6986–7003. <https://doi.org/10.1002/2015JC010818>

Yoder, J. A., Ackleson, S. G., Barber, R. T., Flament, P., & Balch, W. M. (1994). A line in the sea. *Nature*, 371, 689–692. <https://doi.org/10.1038/371689a0>

Carval, T. (2022). Drifting Buoys GDAC Data Management Report 2022. Retrieved from <https://www.ocean-ops.org>

Tables

Buoy ID	Latitude (°)	Longitude (°)	Date of Deployment	Date of Last Transmission	Percentage of data returned	No. of days worked
DB17	12.17	68.70	26-Oct-2024	07-Apr-2025	89.90	163
DB18	19.00	67.24	30-Oct-2024	Not working		
DB20	16.99	68.00	05-Mar-2025	07-Apr-2025	93.50	33
DB21	14.00	68.75	27-Oct-2024	05-Apr-2025	77.08	161
DB22	18.17	67.51	30-Oct-2024	22-Nov-2024	93.47	23
DB23	15.84	68.60	29-Oct-2024	14-Nov-2024	77.62	16
DB24	-1.48	80.47	28-Jul-2024	Not working		
DB25	14.92	68.97	27-Oct-2024	27-Nov-2025	81	30
DB26	17.00	68.14	29-Oct-2024	15-Mar-2025	10.20	137

Table 1: Deployment Details, including Latitude (°), Longitude (°), Date of Deployment, Date of Last Transmission, Percentage of data return, and Number of days worked.

Buoy ID	% Valid After GPS Filtering	% Valid After Speed Filtering	% Valid After SST Filtering	% Valid After BP Filtering
17	97.10%	97.00%	93.00%	90.30%
20	96.70%	96.70%	92.20%	91.30%
21	56.60%	53.80%	51.40%	50.40%
22	96.50%	96.50%	92.10%	90.30%
23	95.00%	95.00%	92.50%	92.90%
25	84.80%	84.80%	73.90%	72.00%
26	74.40%	70.20%	64.00%	53.60%

Table 2: Percentage of valid data retained after successive quality control steps for each drifter buoy. Filtering steps include removal of erroneous GPS positions, unrealistic drift speeds (>3 m/s), and out-of-range and spiky sea surface temperature (SST) and barometric pressure (BP) values.

ID	SST_ Corr	SST RMSD (°C)	SST STD (°C)	MWIR STD (°C)	BP Corr	BP RMSD (hPa)	BP STD (hPa)	ERA5 STD (hPa)
ID17	0.99	0.85	1.08	1.02	0.72	1.58	2.27	1.63
ID20	0.87	0.24	0.46	0.39	0.79	1.55	2.55	1.93
ID21	0.83	0.78	1.28	1.31	0.95	0.89	2.62	2.29
ID22	0.84	0.76	0.21	0.30	0.97	0.32	1.37	1.32
ID23	0.48	0.78	0.15	0.12	0.97	0.37	1.55	1.45
ID25	0.91	0.92	0.84	0.82	0.94	0.55	1.61	1.57

ID26	0.86	1.11	1.33	1.32	0.94	0.60	1.71	1.57
------	------	------	------	------	------	------	------	------

Table 3: Statistical comparison of drifter buoy SST and BP data with MWIR SST and ERA5 BP, showing correlation coefficients, RMSD, and standard deviations for DB17, DB20–DB23, DB25–DB26.

Figures

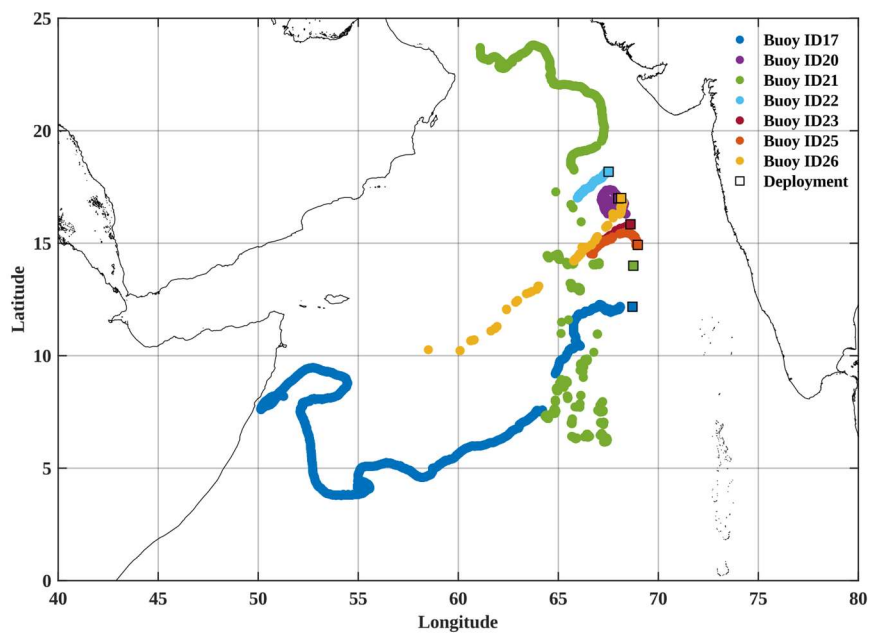


Figure 1: Tracks of 7 drifters (DB17, DB20–DB23, DB25–DB26) marked in different colors, squares marking deployment locations

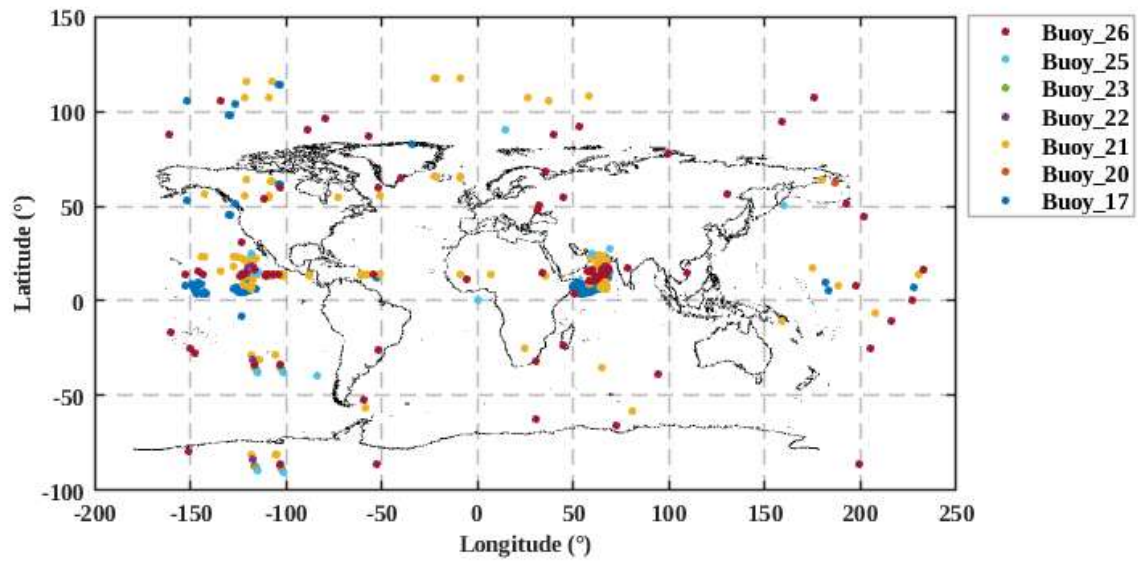


Figure2: initial latitude/longitude data for 7 buoys, with erroneous coordinates on land and non-existent locations

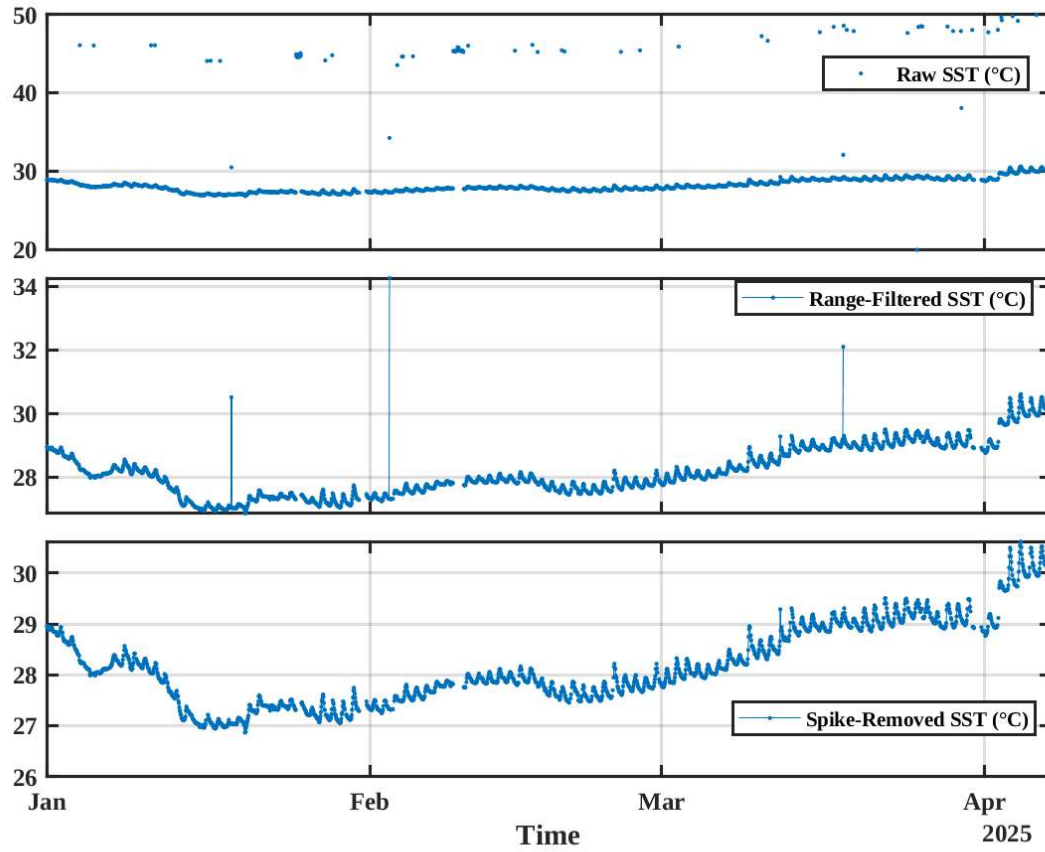


Figure 3. (a) Raw sea surface temperature (SST) data from the drifter, (b) SST after applying range-based filtering to remove values outside the expected physical limits, and (c) SST after final spike removal, showing the cleaned and quality-controlled time series.

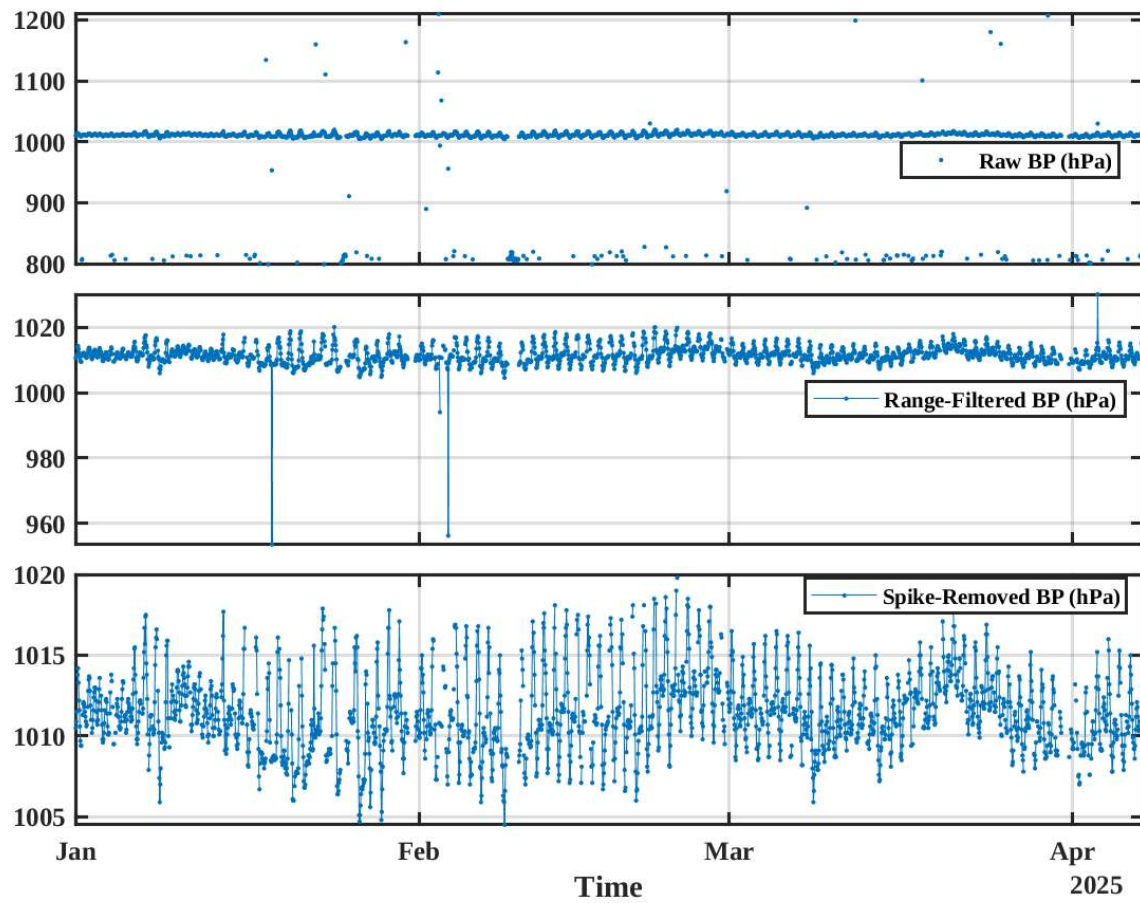


Figure 4. (a) Raw barometric pressure (BP) data from the drifter, (b) BP after applying range-based filtering to exclude physically unrealistic values, and (c) BP after spike removal, resulting in a cleaned and validated pressure time series.

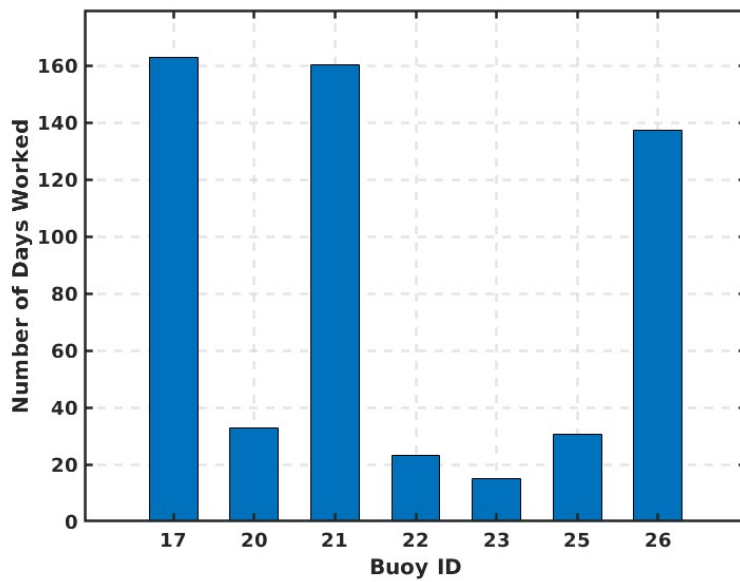


Figure 5. Bar graph showing the number of operational days for each drifter buoy (DB17, DB20–DB23, DB25–DB26), calculated from the deployment date to the last received transmission. The x-axis represents the Buoy ID, and the y-axis indicates the total number of days each unit remained active. DB17, DB20, and DB21 are active as of April 7 2025.

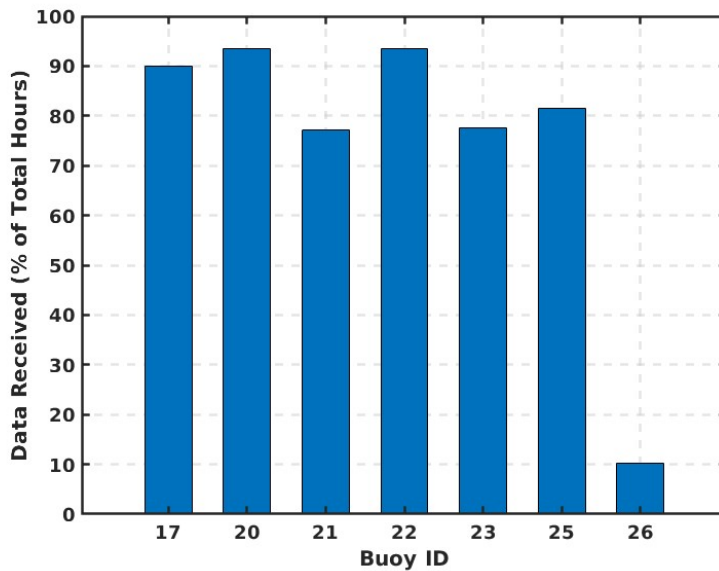


Figure 6. Percentage of data received for each drifter buoy, based on the expected number of hourly transmissions during the respective operational period. The x-axis shows the Buoy ID, while the y-axis represents the percentage of received data relative to the total expected data points.

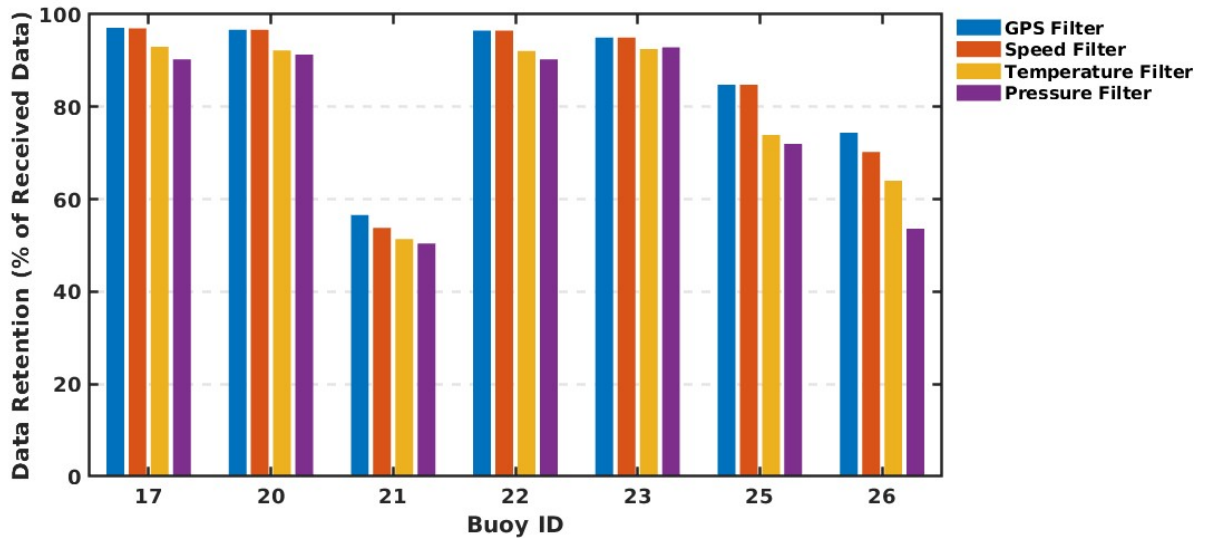


Figure 7: Bar graph showing the percentage of valid data retained after each quality control step for each drifter buoy. The four bars for each buoy ID represent: blue – valid data after GPS filtering, orange – after speed filtering, yellow – after sea surface temperature (SST) filtering, and violet – after barometric pressure (BP) filtering. This visualization corresponds to the values presented in Table 2.

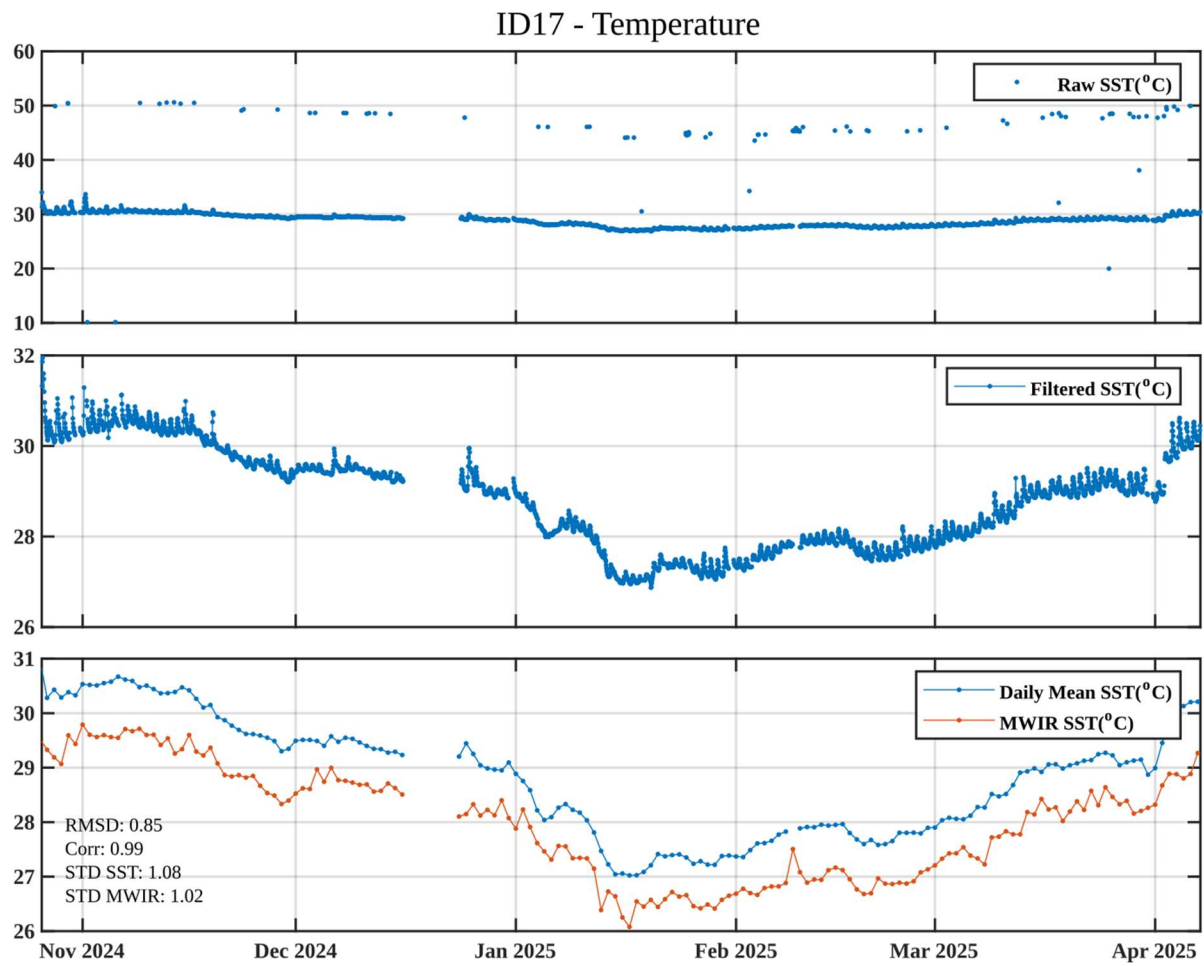


Figure 8. DB17: (a) raw SST, (b) filtered SST after applying range and spike checks, and (c) daily mean SST compared with MW IR SST,

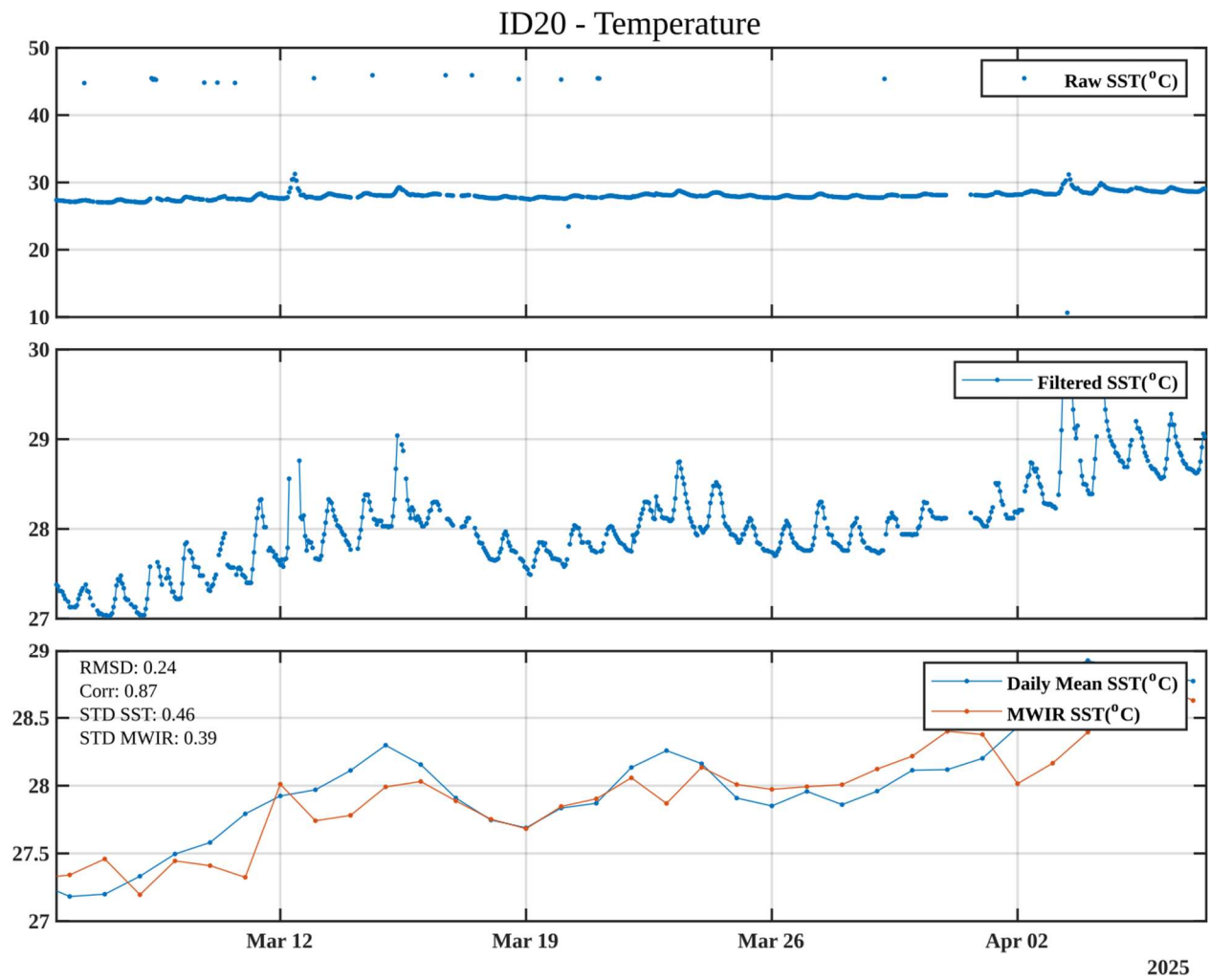


Figure 9: Same as Figure 8 for DB20.

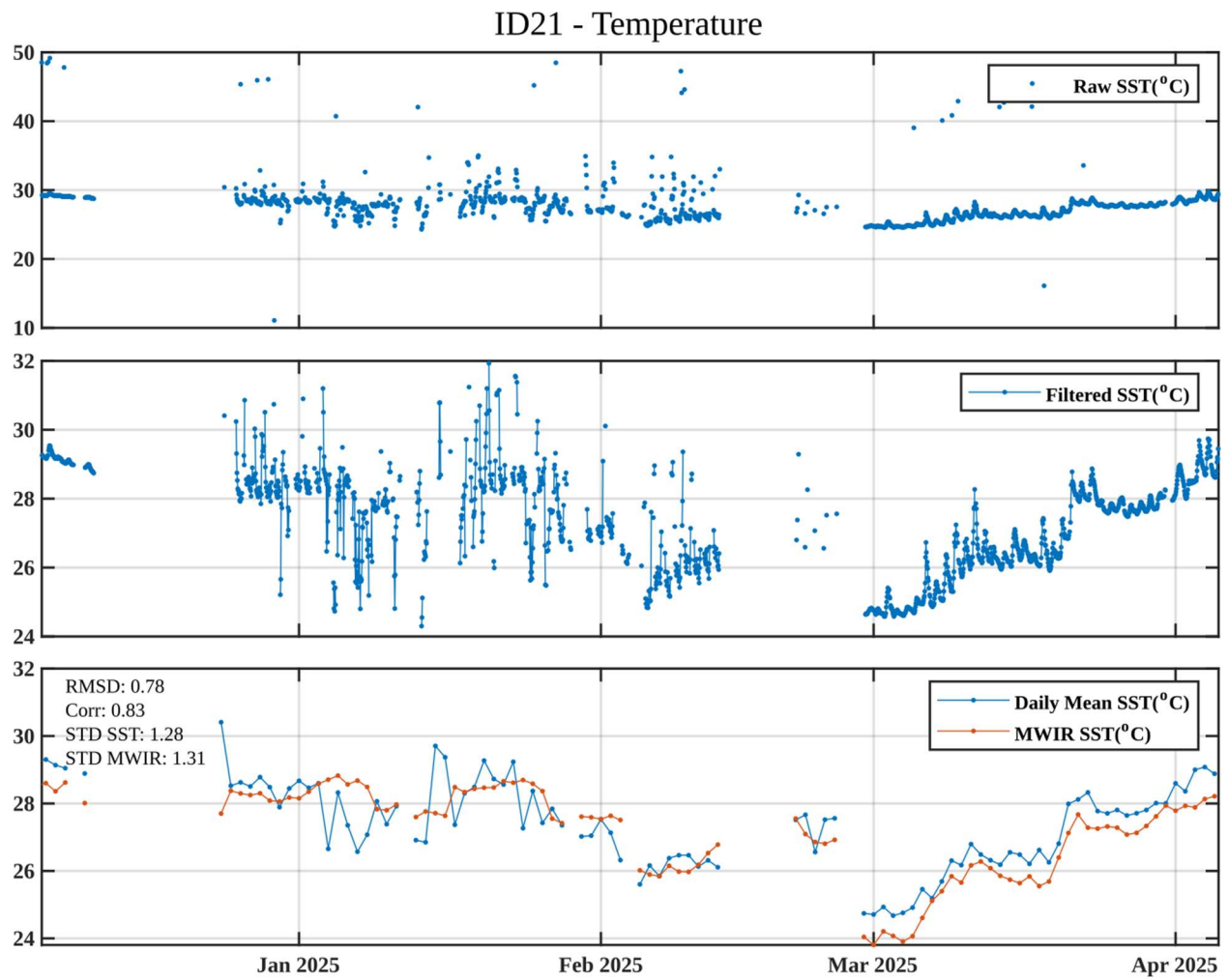


Figure 10: Same as Figure 8 for DB21.

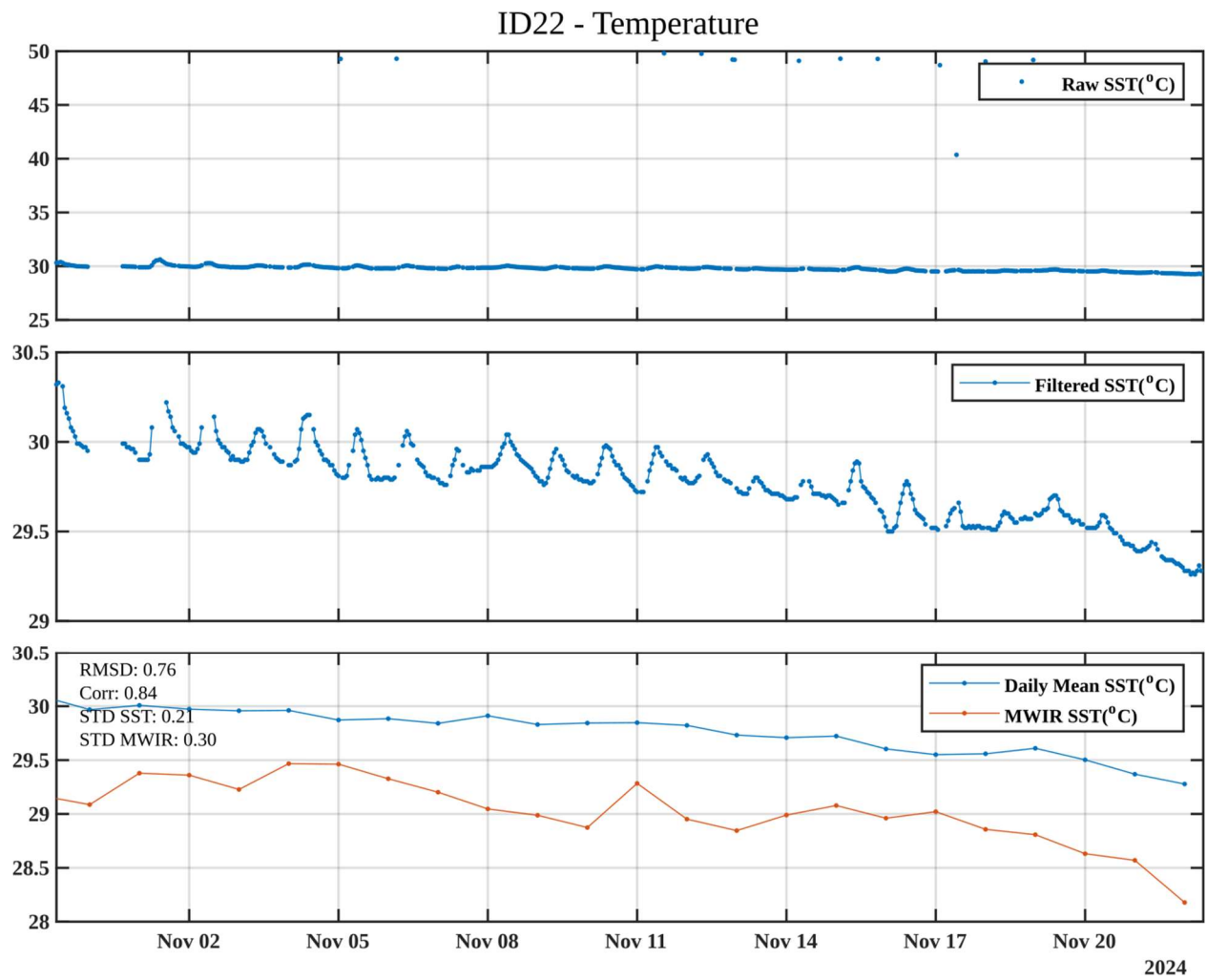


Figure 11: Same as Figure 8 for DB22.

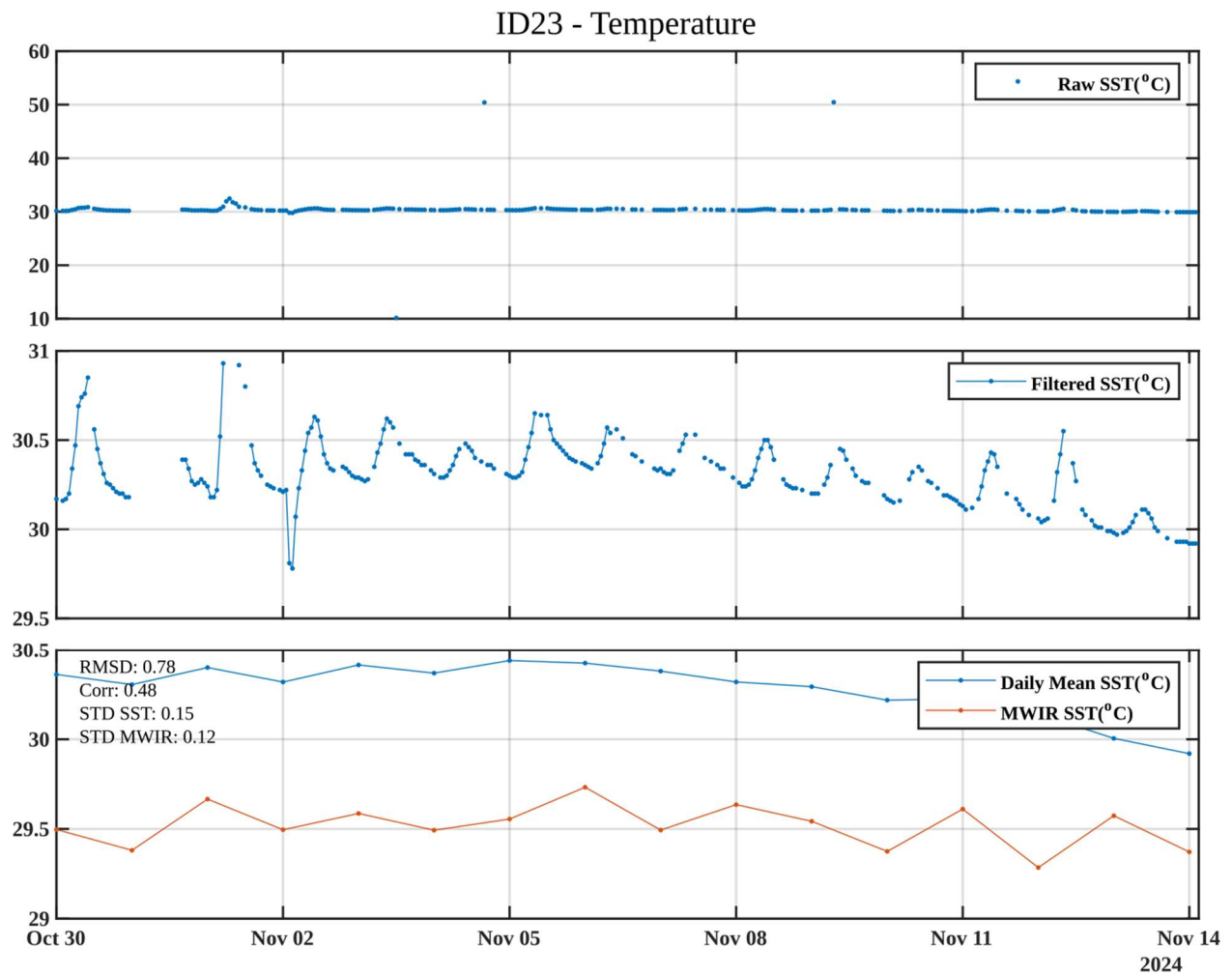


Figure 12: Same as Figure 8 for DB23.

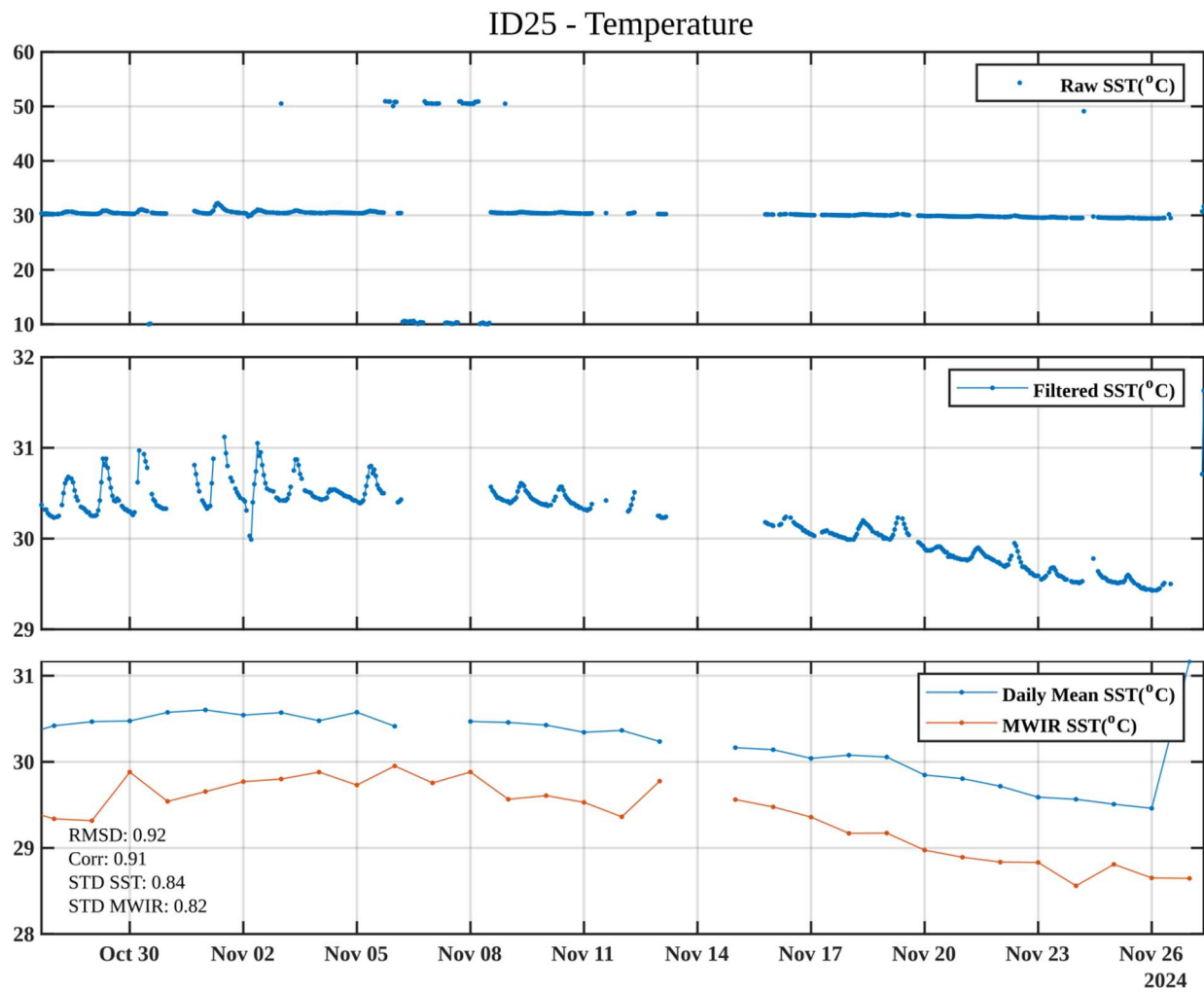


Figure 13: Same as Figure 8 for DB25.

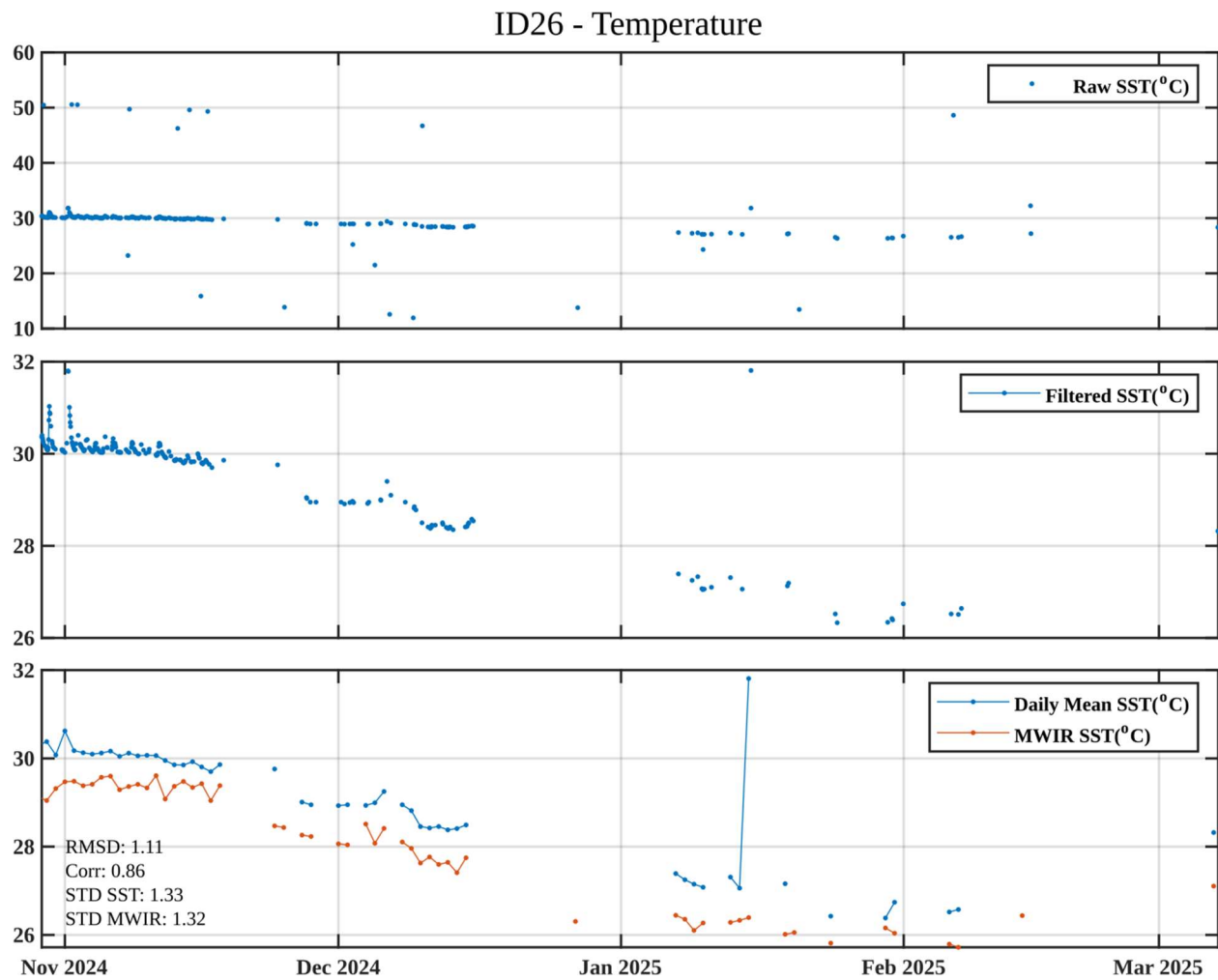


Figure 14: Same as Figure 8 for DB26.

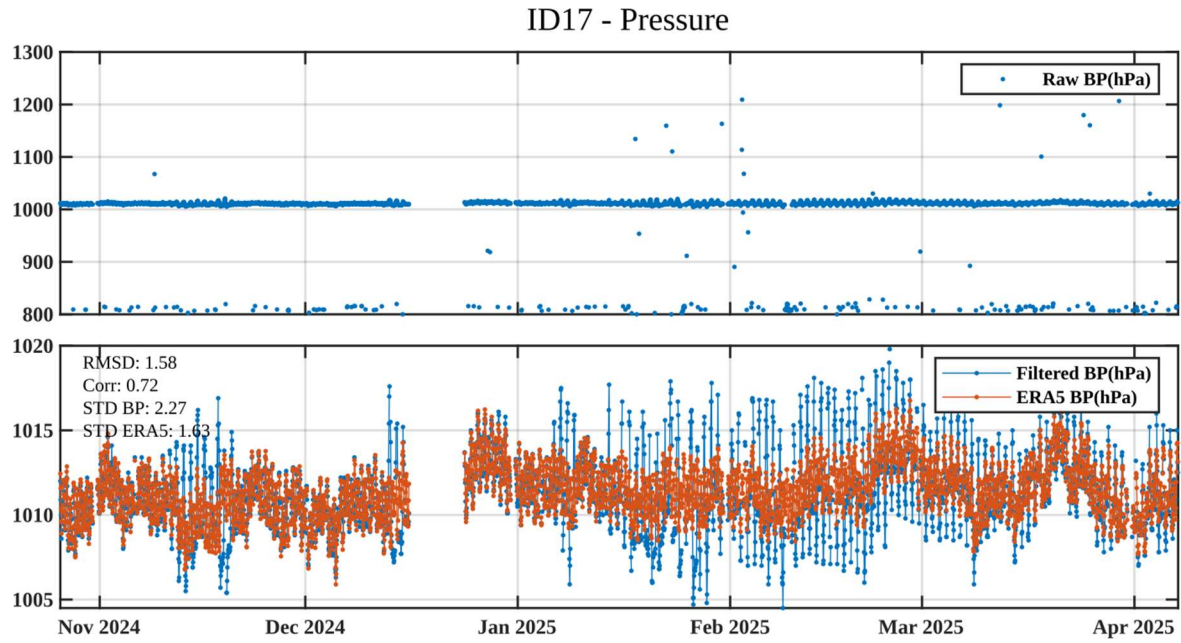


Figure 15: DB17, a) Raw barometric pressure (BP) data, b) Filtered BP (blue) compared with ERA5 reanalysis (orange line).

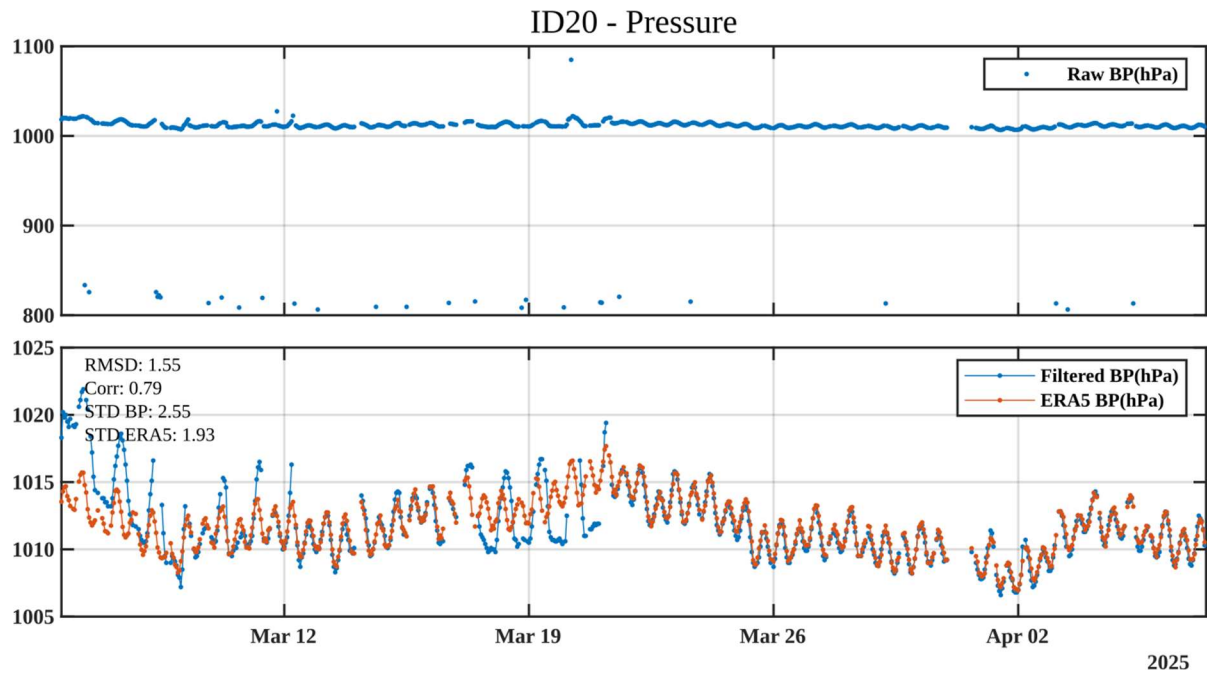


Figure 16: Same as Figure 15 for DB20.

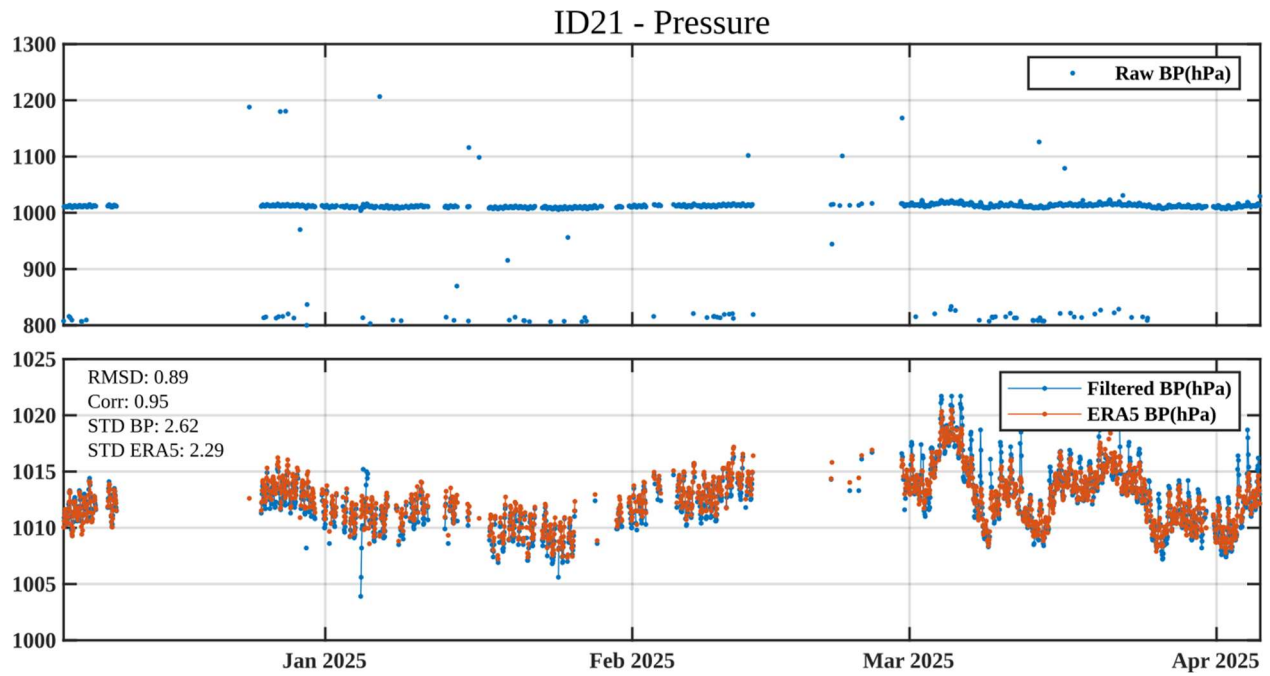


Figure 17: Same as Figure 15 for DB21.

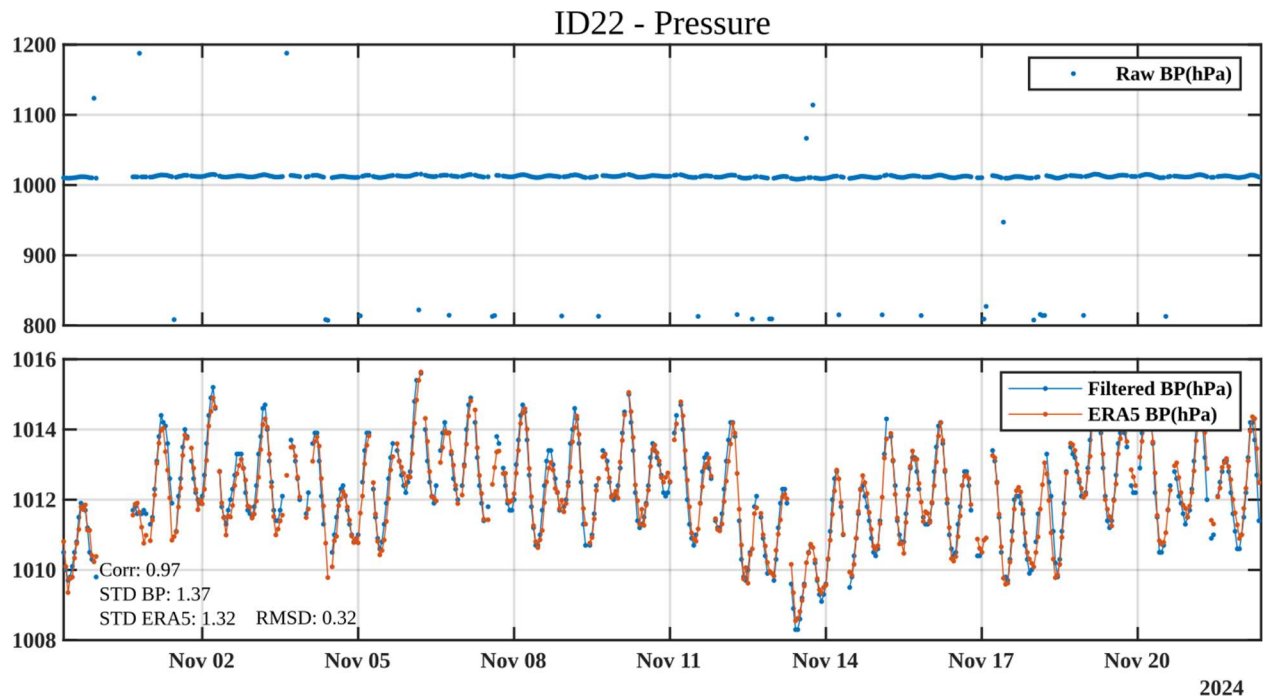


Figure 18: Same as Figure 15 for DB22.

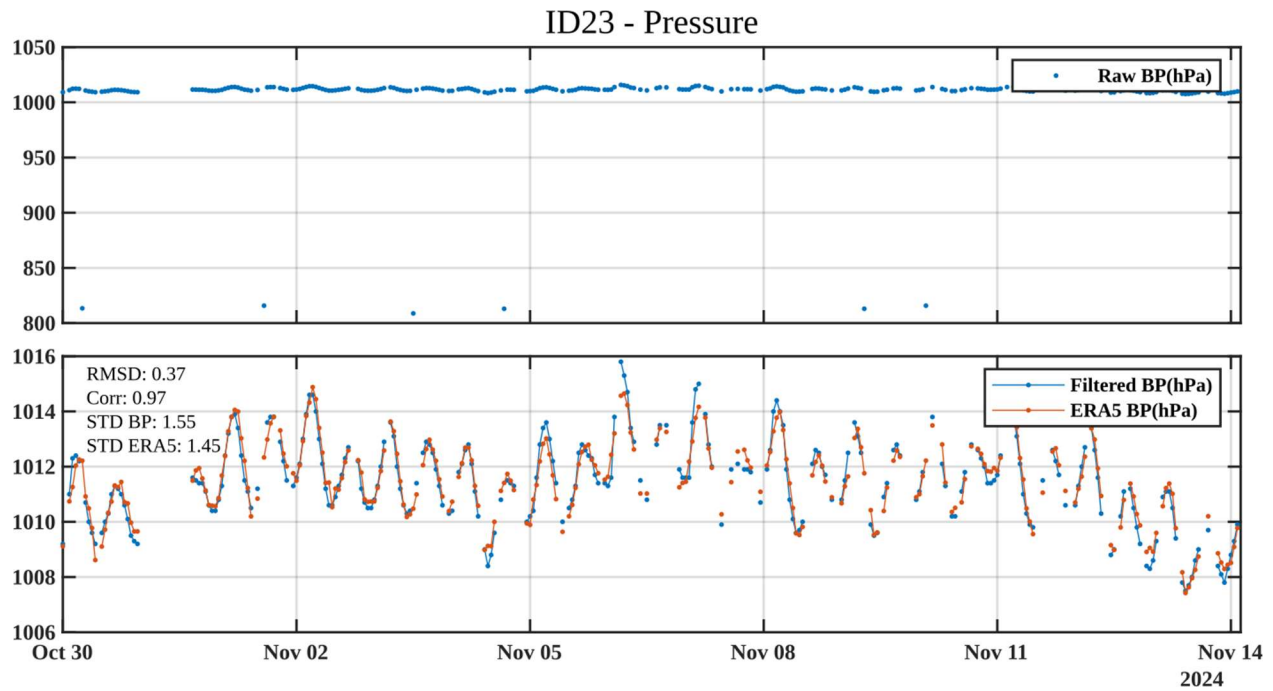


Figure 19: Same as Figure 15 for DB23.

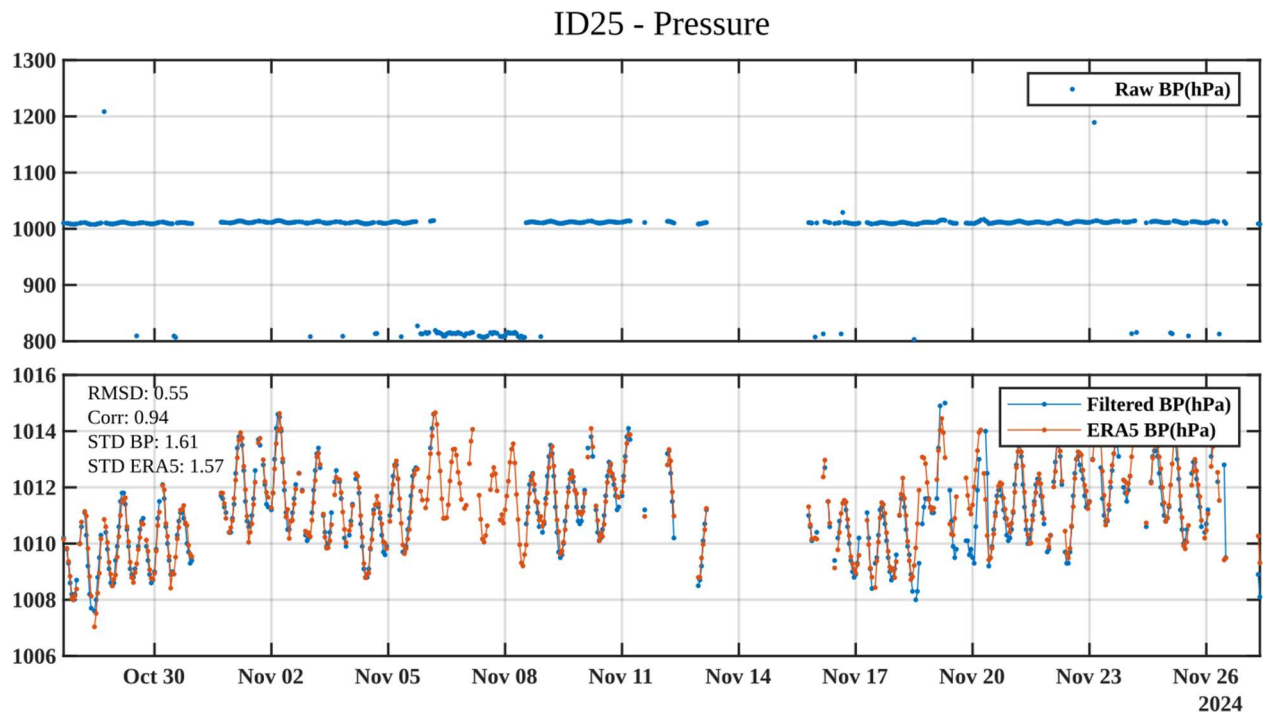


Figure 20: Same as Figure 15 for DB25.

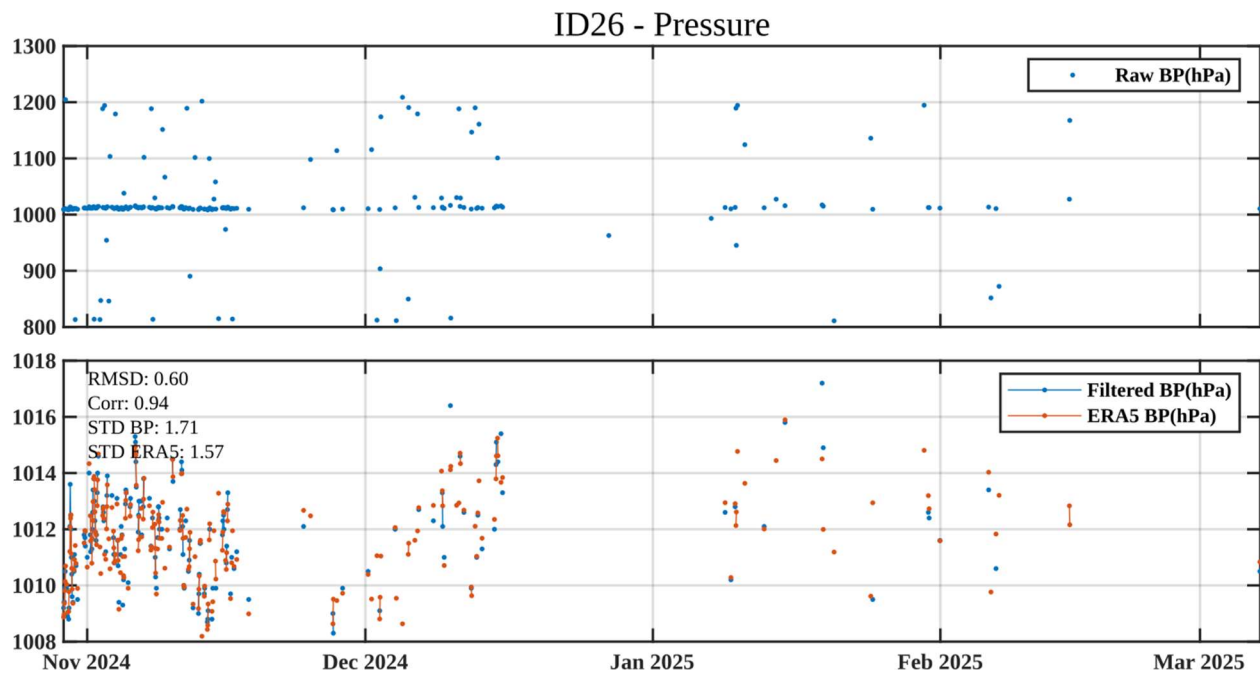


Figure 21: Same as Figure 15 for DB26.